NASA CONTRACTOR REPORT

NASA CR-1165

NASA CR-1165

AMPTIAC

MECHANISM OF THE ATMOSPHERIC INTERACTION WITH THE FATIGUE OF METALS

by M. J. Hordon and M. A. Wright

Prepared by
NORTON RESEARCH CORPORATION
Cambridge, Mass.
for

NATIONAL AERONAUTICS AND SPACE ADMINISTRATION • WASHINGTON, D. C. • SEPTEMBER 1968

NASA CR-1165

MECHANISM OF THE ATMOSPHERIC INTERACTION WITH THE FATIGUE OF METALS

By M. J. Hordon and M. A. Wright

Prepared under Contract No. NASw-1533 by
NORTON RESEARCH CORPORATION
Cambridge, Mass.

for

NATIONAL AERONAUTICS AND SPACE ADMINISTRATION

For sale by the Clearinghouse for Federal Scientific and Technical Information
Springfield, Virginia 22151 – CFSTI price $3.00

FOREWORD

This Summary Report covers the work performed by Norton Research Corporation for the Office of Advanced Research and Technology, National Aeronautics and Space Administration under Contract No. NASw-1533 during the period January 3, 1967 to January 3, 1968. The program is a continuation of a series of investigations to determine the effect of vacuum and low partial gas pressure environments on the fatigue properties of metals conducted under previous NASA Contracts Nos. NASw-962 and NASw-1231.

The major contributors to this program were Dr. M. J. Hordon, Program Director and Principal investigator, and Dr. M. A. Wright, Senior Metallurgist of the research staff of NRC. The program was under the general supervision of Dr. N. Beecher, Assistant Director of Research for NRC. The NASA technical monitor was Mr. R. Raring, OART, NASA, Code RRM.

Some of the results of this program have been published or are in process of publication in the technical literature.[1,2]

TABLE OF CONTENTS

MECHANISM OF THE ATMOSPHERIC INTERACTION WITH THE FATIGUE OF METALS

by M. J. Hordon and M. A. Wright

SUMMARY

This report presents the results of an investigation continuing an examination of the fatigue properties of aluminum in vacuum. In the current phase, experimental work was directed at cyclic frequency and tensile fatigue effects and at the defect substructure generated in vacuum by fatigue stressing.

The mean fatigue life was observed to depend on the cyclic rate of straining at all pressure levels. However, in the region of the critical pressure zone for fatigue life enhancement, changes in the cyclic frequency were noted to have a major effect on crack propagation, an increase in cyclic straining rate acting to shift the transition level to higher pressures.

Measurements of the fatigue life under conditions limited to alternating tensile stresses alone showed that fatigue life enhancement or crack growth retardation in vacuum was not dependent on compressive stress distributions or fatigue crack closure. The experimental work inferred that crack retardation should not be mainly attributed to the reweldment of fracture surfaces in vacuum, but may be produced by dislocation glide and escape at oxide-free surfaces to reduce internal stresses.

Finally, a well defined correlation was observed between the fatigue properties of aluminum and dislocation substructural distributions revealed by thin film electron microscopy. Under conditions of repeated loading, subgranular dislocation arrays were formed with an average size dependent on the strain amplitude and the prior dislocation distribution.

MECHANISM OF THE ATMOSPHERIC INTERACTION WITH THE FATIGUE OF METALS

by M. J. Hordon and M. A. Wright

INTRODUCTION

As noted in detail in previous summary reports issued in this series[3,4] and in derived publications,[5,6] the rate of fatigue failure, measured as the number of strain cycles to nucleate and propagate a crack through a specimen, was found to depend markedly on the gaseous environment surrounding the specimen. In particular, for partial pressures of oxygen and water vapor depleted below a critical level dependent on the strain amplitude, cyclic frequency and temperature, a marked retardation in the rate of fatigue crack growth corresponding to an increase in the fatigue life was observed compared to the normal rate in air or in oxygen/water vapor-rich environments.

The transition in the crack growth rate was observed to occur within a well defined low pressure zone, denoted as the critical pressure zone, generally about 10^{-2} to 10^{-4} torr for fatigue tests of 1100 aluminum at 20°C and cyclic rates below 50 cycles/sec. The implication of these results on the reduced pressure dependence of the fatigue behavior of aluminum for space application is apparent. In the high vacuum environment of space, well below 10^{-4} torr, the extremely low concentrations of O_2 and H_2O gas molecules should act to increase the resistance to fatigue failure, compared to normal earth atmosphere, of periodically stressed spacecraft components and elements.

An explanation for the relatively sharp change in fatigue crack growth characteristics in the neighborhood of the critical pressure zone was advanced previously[5] in terms of competing rates of crack extension and oxide adsorption at the base of the

crack. Estimates of the rate of molecular O_2 or H_2O transport and adsorption with a long, narrow crack geometry were found to be equivalent to the actual rate of crack extension at the critical pressure. At higher pressure levels, the rate of adsorption would be expected to exceed the rate of production of new crack surfaces. Hence the fatigue crack surface would be continuously saturated and an adherent oxide film quickly formed. At vacuum levels below the critical zone, it can be anticipated that the crack front would propagate via internal stress concentrations faster than the adsorption rate; hence newly formed crack surfaces would remain uncontaminated and the enhancing effect of an oxide film on the rate of extension be avoided.

In the previous investigations of this series, efforts were directed to test the adsorption rate hypothesis by studying the fatigue behavior of pure aluminum under various conditions. The following results may be briefly summarized:

1. Observations of the number of strain cycles to nucleate and to propagate visual fatigue cracks in vacuum and in air showed that the nucleation life was substantially the same in both environments; the major change was the decrease in crack growth rate in vacuum. Hence the fatigue effect could be attributed to the interaction of the gaseous medium and the crack.

2. Measurements of the fatigue life of aluminum through the low pressure range down to 5×10^{-11} torr[1] have shown that the major enhancement of fatigue resistance occurred in the vicinity of the critical pressure zone; relatively little further change was noted at lower pressures. This observation reinforces the adsorption concept, since at all pressure levels below the critical, the rate of fatigue crack propagation should be relatively independent of residual gas pressure.

3. Measurements of the effect of residual gas concentrations on the fatigue behavior were carried out for highly purified species including oxygen (O_2), water vapor (H_2O) and hydrogen (H_2) in the partial pressure range 10^{-6} to 10^{1} torr. The results showed that the crack growth rate was influenced by both O_2 and H_2O residual contents at partial pressures about 10^{-2} - 10^{-3} torr. Pure H_2 had relatively no effect on the fatigue properties. The inference of this data is that the crack growth rate was sensitive to the rate of oxide adsorption in the crack.

4. Measurements of the effect of temperature, cyclic strain frequency and strain amplitude level showed that the critical pressure for the transition in crack propagation rate could be shifted in accordance with changes in the intrinsic rates of crack extension and oxygen adsorption.[5,6] Thus, an increase in temperature from 20 to 100°C decreased the adsorption rate and resulted in raising the critical pressure to approximately 10^{-2} torr. In the same manner, increases in the cyclic rate and strain amplitude raised the critical pressure by increasing the intrinsic crack extension rate.

As a result of these investigations, it was concluded that the rate of fatigue crack propagation in 1100 aluminum was sensitive to the formation of adherent oxide films on newly exposed fracture surfaces at the crack tip. Two mechanisms have been proposed to explain this phenomenon; (1) rewelding of clean, oxide-free crack interfaces during cyclic compression and, (2) stress relieval by the adsorption of plastically induced defects such as dislocations at uncontaminated free surfaces. In these mechanisms, the formation of an adherent oxide film both prevents rewelding and forms a barrier to dislocation escape, thus acting to enhance the conditions for further crack growth.

For the current investigation, two aspects of the fatigue mechanism at low pressure were selected for further study. In an initial phase of the program, it was decided to examine in more detail the effect of cyclic frequency on fatigue behavior since it has an important influence on the adsorption mechanism and the critical pressure zone.

In a second phase, an experiment was proposed to test the crack rewelding mechanism advanced to explain crack growth retardation at low pressures. Since the rewelding concept should require fracture surface recontact and hence crack compression in order to promote bonding, a test was devised in which the fatigue crack, once formed, would be held continuously under tension and cycled with a tensile stress amplitude. The test procedure would be similar to a tensile-release periodic stress mode with a non-zero minimum stress. In this manner, the crack propagation behavior in vacuum could be examined under conditions which would minimize the possibility for extensive crack rewelding.

In a final phase of the program, an examination of the substructural mechanism of fracture in vacuum was proposed for comparison with established mechanisms in air. In this portion of the work, the effect of strain amplitude and prior induced plastic deformation on subgranular formation, dislocation multiplication and crack extension was to be studied by means of electron microscopy in an environment in which the intrinsic mode of fracture advancement could be separated from the corrosive enhancement of oxygen adsorption.

PHASE I

CYCLIC FREQUENCY EFFECTS

INTRODUCTION

As noted previously, fatigue tests of 1100-H14 aluminum were carried out in reverse bending at constant flexure amplitudes to produce surface strains in the range 1.2-1.9 x 10^{-3} in./in.[3] The tests were performed in the Unit I assembly through a pressure interval extending from atmospheric (7.6 x 10^{2} torr) to about 2 x 10^{-7} torr. Comparative tests conducted at cyclic strain frequencies of 25 and 50 cycles/sec showed evidence that both the cyclic life to fracture and the critical pressure for the fatigue crack growth transition increased with frequency.

In order to examine this effect in greater detail, additional reverse bending fatigue tests were scheduled for the current investigation. It was planned to perform constant flexure tests both in Unit I, with a low pressure limit of 2 x 10^{-7} torr and a cyclic frequency range of 0 to 50 cycles/sec, and in the XHV Unit II, capable of attaining pressures below 10^{-10} torr with a cyclic frequency range of 50 to 150 cycles/sec. The tests were planned at relatively low surface strain amplitude levels designed to produce fracture lives in the range 2 to 5 x 10^{5} cycles in normal atmosphere. High stress-strain amplitude levels producing cyclic lives less than 10^{5} cycles would tend to obscure frequency effects by narrowing the scatter in the fracture life band. Lower stress-strain levels yielding cyclic lives greater than 10^{6} would require extremely long test schedules with little further gain in frequency sensitivity.

Furthermore, in order to maximize any detectable frequency effect, and to minimize the influence of general fatigue scatter, widely varying cyclic fatigue ratios were selected. For Unit I tests, cyclic frequencies of 10 and 50 cycles/sec were chosen yielding a frequency differential of 5 to 1. For the XHV Unit II tests, the maximum frequency differential was 50 to 150 cycles/sec or 3 to 1.

EXPERIMENTAL PROCEDURE - PHASE I

The fatigue test units designated Unit I and Unit II have been described in detail in previous reports.[3,4] Unit I consisted of a massive stainless steel vacuum flange plate and base which capped a cylindrical vacuum chamber evacuated by a 400 lit/sec ion pump as shown in Fig. 1. The cantilever-type specimens were radially fastened at one end to the base as shown in Fig. 2. The other end was attached to an eccentrically driven crank rod connected to the flange plate by a flexible bellows seal. Eight concentric independent test stations were provided powered by separate 1/15 H.P. electric motors as shown in Fig. 3. Constant strain amplitudes in the range 1.2 to 1.9 x 10^{-3} were provided by a series of eccentric bearing assemblies.

Unit II, described in detail previously,[1] consisted of cylindrical power system and frame designed to be incorporated in the Extreme High Vacuum (XHV) System previously developed at NRC. As shown in Fig. 4, an annular frame supported the fixed outer end of eight cantilever-type specimens radially mounted in the unit. The inner ends of the specimens were connected to a central shaft vibrated by an electromagnetic exciter. The exciter unit was enclosed in a stainless steel fixture in order to permit air cooling. The drive shaft was carried into the high vacuum region

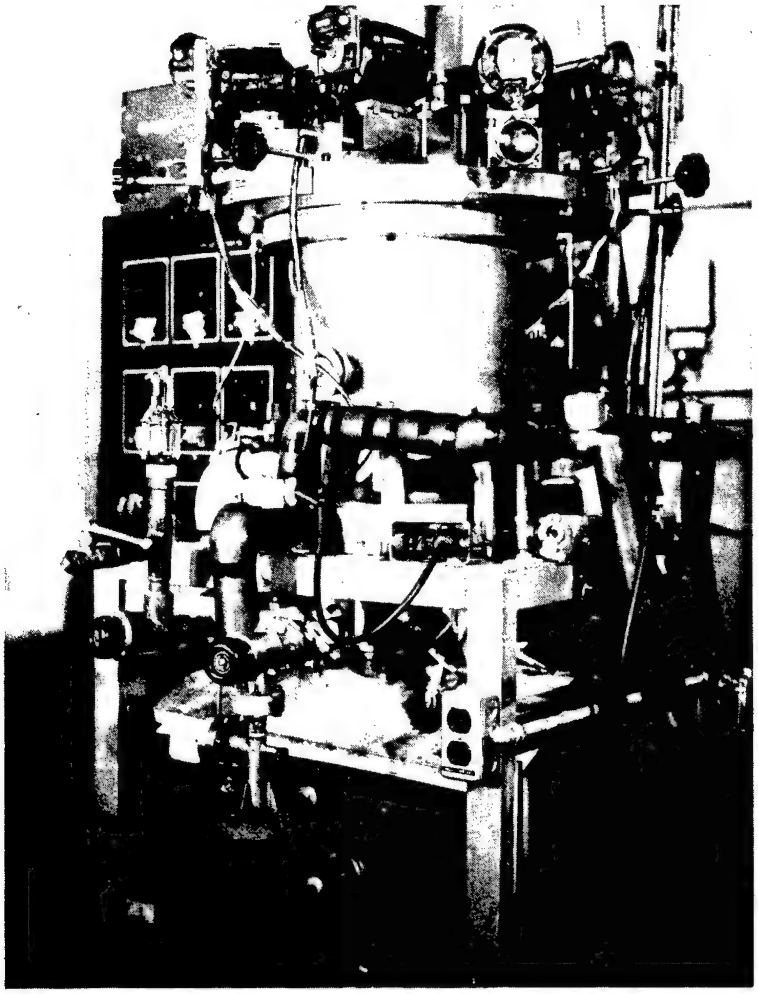

View of Unit I Fatigue Apparatus

Fig. 1

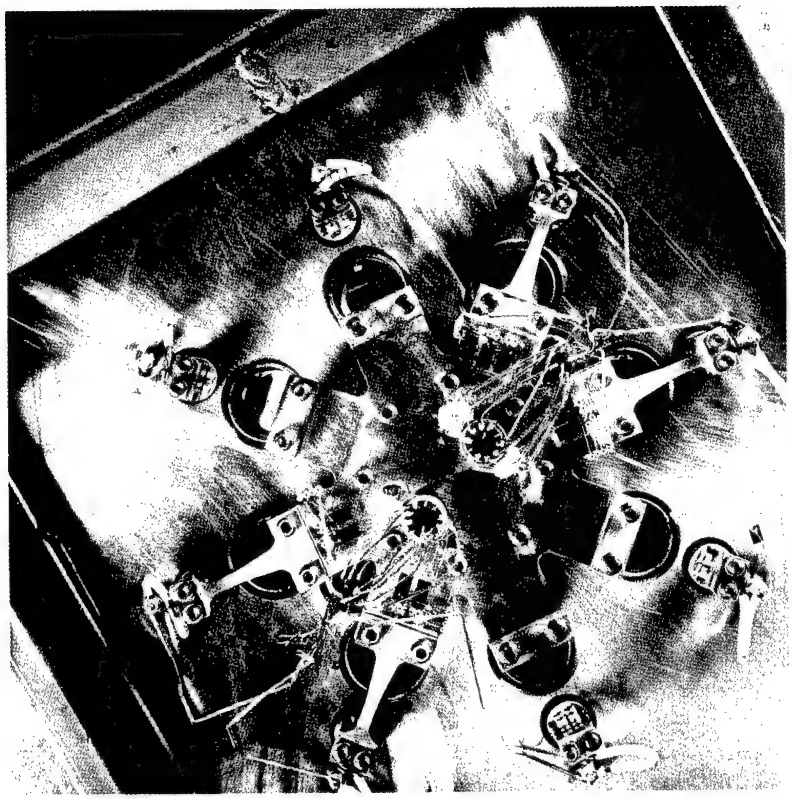

Bottom View of Vacuum Fatigue Base Flange Unit

Fig. 2

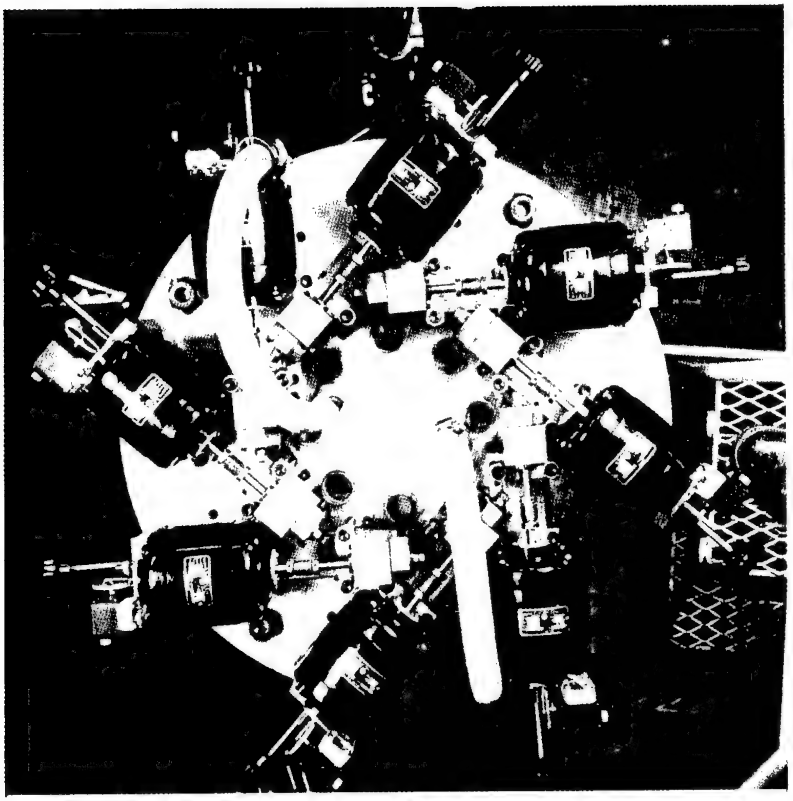

Top View Of Fatigue Unit I Vacuum Flange Showing Motor Drive and Bearing Housing Assemblies.

Fig. 3

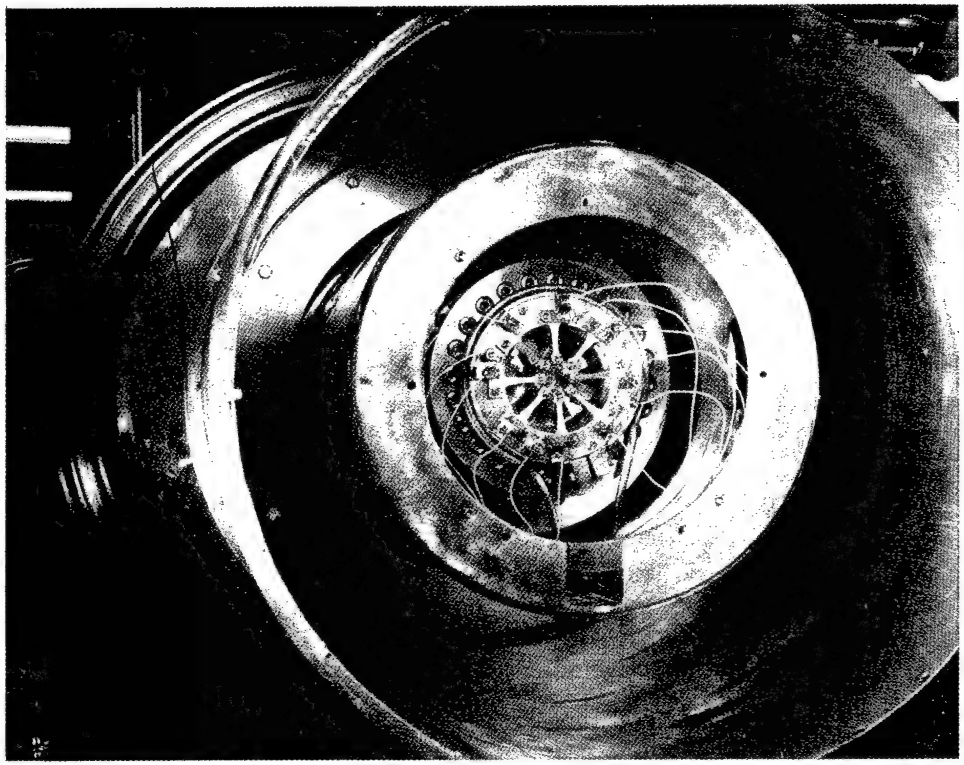

View of Fatigue Apparatus Unit II In XHV System

Fig. 4

by means of a concentric triple bellows assembly which compensated for the pressure gradient and provided an interim guard vacuum between the pressure extremes. The vibration amplitude was controlled by a sensitive electronic feed back circuit comprising an array of ceramic bonded resistance strain gauges as the sensing element. The reverse bend specimen configurations for both test units are illustrated in Fig. 5.

Deflection amplitudes with the bearing eccentrics in Unit I were maintained within $\pm$ 2 x 10^{-4} in. for total deflections of $\pm$ 25 - 40 x 10^{-3} in.; in Unit II, the control circuit maintained total flexures of $\pm$ 20 - 35 x 10^{-3} in. within $\pm$ 1 x 10^{-3} in.

In fatigue test operation, pressure levels in Unit I in the range 10^{-4} to 2 x 10^{-7} torr were attained by an ion pump using a series of orifice plates at the evacuation port. Pressures above 10^{-4} torr were generated by mechanical pumping. In Unit II, extremely low pressures down to 5 x 10^{-11} torr were achieved by a cryopumping procedure, with the indicated pressures recorded by an NRC Redhead cold cathode Magnetron gauge.

Multiple fatigue tests were conducted at selected flexure amplitude levels in both apparatus in order to reduce statistical scatter in fracture life and pressure level. The number of strain cycles to fracture were determined in Unit I by counters recording motor revolutions and in Unit II by the elapsed time until fracture. The time-to-fracture was monitored by a relay circuit which stopped each individual station time recorder upon physical separation of the specimen.

EXPERIMENTAL RESULTS - PHASE I

Fatigue tests were conducted in Unit II using polished cantilever-type specimens as shown in Fig. 5. Simultaneous

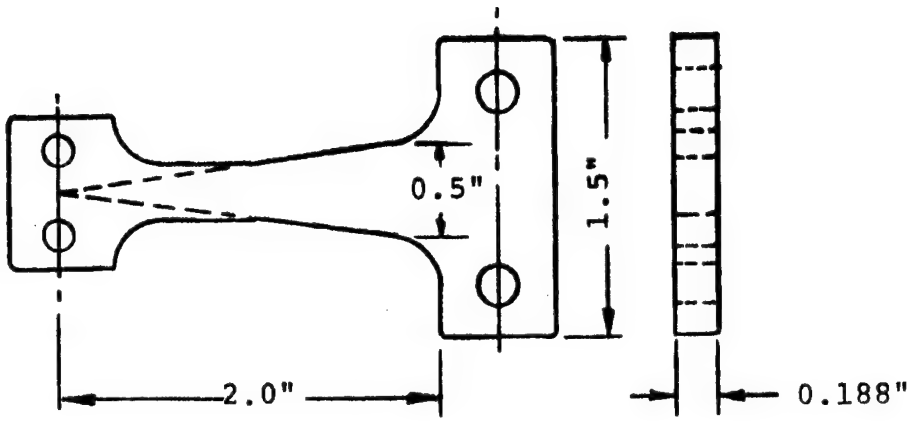

(a) Flexure fatigue specimen for Unit I

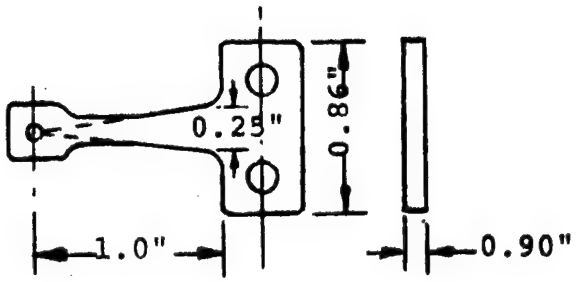

(b) Flexure fatigue specimen for Unit II

Fig. 5 Specimen geometries for fatigue tests in Reverse Bending.

tests of eight specimens were performed in air at normal atmosphere and at vacuum levels about 1×10^{-10} torr at cyclic frequencies of 50 and 150 cycles/sec. With a standard deflection amplitude of $\pm$ 0.016 in. corresponding to a surface strain amplitude of $\pm 1.4 \times 10^{-3}$, fracture lives in the range $1.5 - 5.0 \times 10^{5}$ cycles were usually observed in air.

The effect of a three-fold change in cyclic bending rate at one atmosphere and 10^{-10} torr on the fracture life of 1100 aluminum at a standard strain amplitude of $\pm 1.4 \times 10^{-3}$ is indicated in Table I. It is evident that an increase in the mean fracture life was observed both with an increase in bending rate and with a decrease in the pressure. However, the effect of frequency on the mean cyclic life at any constant pressure level was relatively small, reaching a maximum of approximately 25 per cent at 10^{-10} torr. In comparison, the increase in cyclic life with reduced pressure was about 250 per cent.

Additional fatigue tests were conducted at the same strain amplitude level in Unit II through the reduced pressure range $10^{0} - 10^{-3}$ torr by mechanical pumping in combination with a controlled leak rate with the object of examining the frequency effect in more detail. The results are shown in Fig. 6 in which the mean fracture life dependence on pressure level is plotted for tests at 50 and 150 cycles/sec. It is apparent that the results initially obtained at one atmosphere and 10^{-10} torr are consistently maintained through the critical pressure interval for the transition in fatigue behavior. It may be noted that the magnitude of the fracture life increase obtained with increasing the bending rate from 50 to 150 cps is relatively stable for pressure levels below a critical level about 10^{-2} torr.

It may be noted that the variation in fatigue life with cyclic bending rate underwent a marked change in the critical

TABLE I

COMPARATIVE EFFECT OF CYCLIC LOADING FREQUENCY ON FATIGUE FRACTURE LIFE

PRESSURE (torr)	SPECIMEN	FRACTURE CYCLES ($N \times 10^5$) 50 cps	150 cps
7.6×10^2	1	1.15	1.23
	2	1.21	1.40
	3	1.31	1.45
	4	1.32	1.59
	5	1.34	1.64
	6	1.35	1.64
	7	1.36	1.62
	8	1.50	1.74
	mean	1.33	1.54
1×10^{-10}	1	2.59	2.89
	2	2.82	3.28
	3	3.04	3.78
	4	3.04	4.16
	5	3.19	4.41
	6	3.21	4.50
	7	3.24	5.17
	8	3.75	5.25
	mean	3.13	4.15

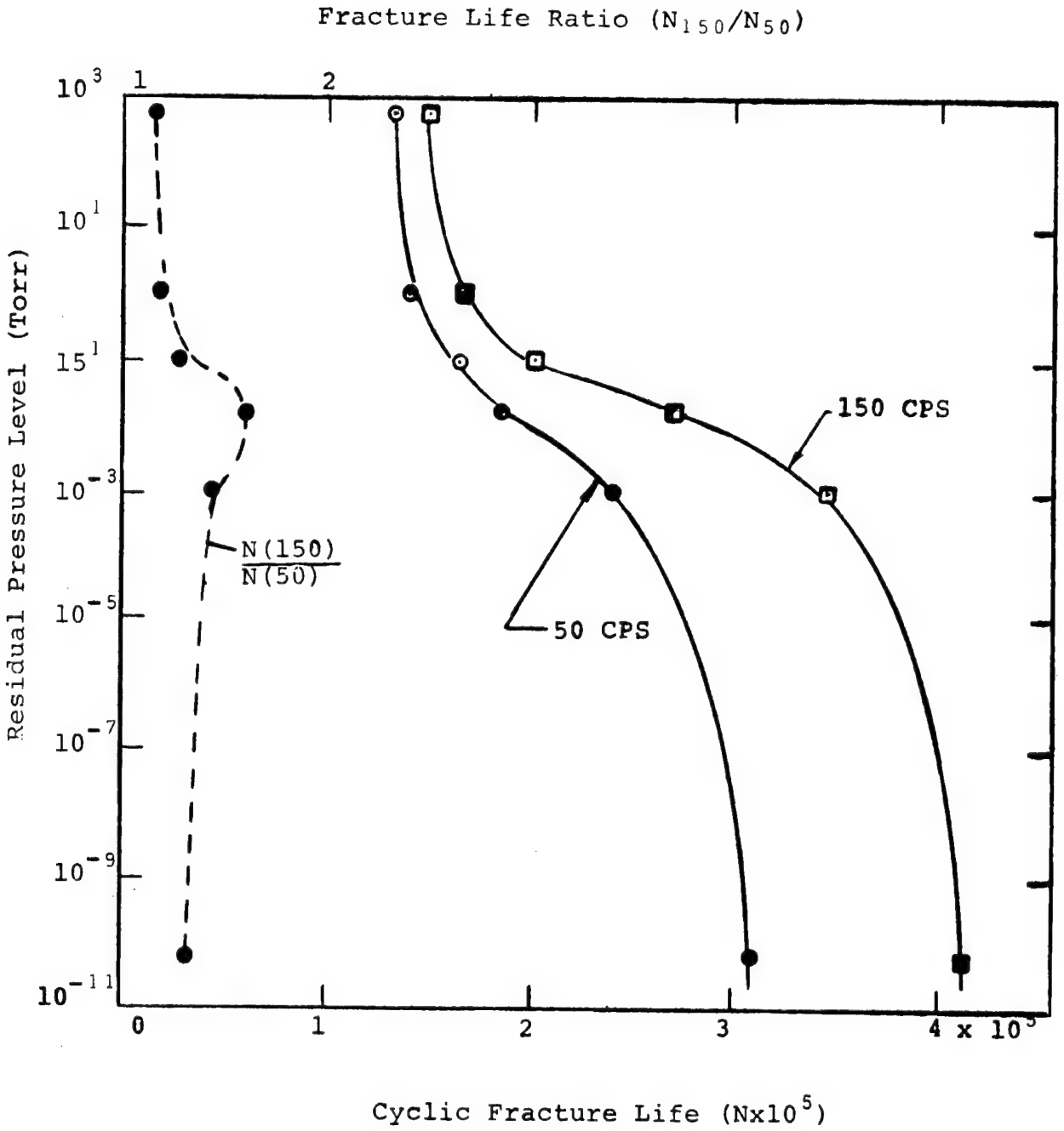

Fig. 6 Cyclic loading rate dependence of fatigue life of 1100 aluminum at reduced pressure levels in Unit II tests.

pressure zone. The ratio of the fracture life at 150 cycles/sec to 50 cycles/sec increased from a value of 1.25 at 10^{-1} torr to a maximum value of about 1.59 at 2×10^{-2} torr. The ratio thereafter decreased steadily, yielding values of 1.42 at 10^{-3} torr and 1.32 at 10^{-10} torr. As shown in Fig. 6, a significant change in fatigue life with bending rate was found to occur in the critical pressure zone extending from 10^{-1} to 10^{-3} torr. At pressure levels above or below this zone, the frequency effect was substantially less.

To correlate with the cyclic rate effect in the critical pressure zone found in the Unit II tests, an additional series of fatigue tests were scheduled for Unit I. In these tests, the fatigue properties of 1100-H14 aluminum were determined in reverse bending at a constant surface strain amplitude of $\pm$ 1.2 x 10^{-3} to produce fatigue fracture in the cyclic range 6 - 10 x 10^5 cycles in air. Bending rates of 10 and 50 cycles/sec were chosen to maximize any observable rate effect. Similarly to the tests in Unit II, multiple tests were performed under equivalent conditions to reduce the scatter. However, in the Unit I tests, four of the available stations were run at 10 cycles/sec and the remaining four at 50 cycles/sec in each vacuum operation in order to accentuate the effect of cyclic rate on the fracture life under conditions of identical vacuum levels.

The experimental results for the Unit I fatigue tests are given in Fig. 7. It is evident that the influence of cyclic loading rate was generally similar to the data obtained in the Unit II tests. The maximum cyclic rate effect occurred in the transitional pressure zone extending from about 10^{-1} to about 10^{-4} torr as evidenced from the increase in the fracture life ratio. The maximum value of the ratio was approximately 2.04 at 10^{-2} torr compared to values of about 1.40 at both unit atmosphere (7.6×10^2 torr) and 5×10^{-5} torr.

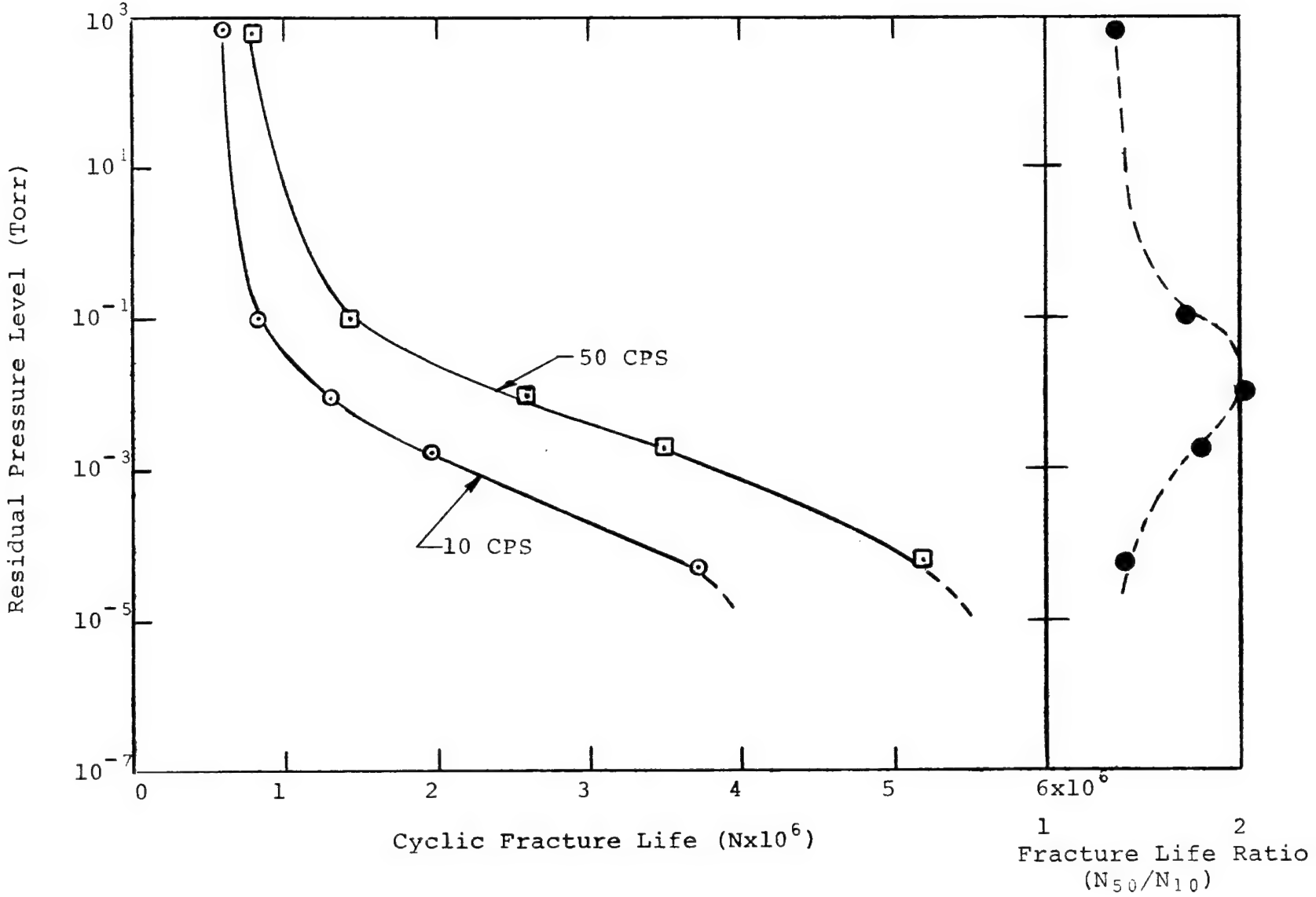

Fig. 7 Cyclic loading rate dependence of fatigue life of 1100 aluminum at reduced pressure in Unit I tests.

DISCUSSION - PHASE I

It is apparent from the results shown in Figs. 6 and 7 that the cyclic fracture life produced by reverse bend flexure tests at constant deflection was measurably dependent on the frequency of cyclic loading at all pressure levels including atmospheric. These results are in general accord with a wide body of experimental evidence showing moderate increases in cyclic fatigue life with increased cyclic frequency.[7] The present data suggest that this frequency effect will persist at reduced pressure levels.

Moreover, the present results indicated that a marked, discontinuous change in fatigue life with frequency was superimposed on the general increase in the neighborhood of the critical pressure zone extending from about 10^{-1} to 10^{-4} torr. The frequency effect associated with the critical pressure band can be most clearly distinguished by plots of the ratio of the cyclic fracture lives at two frequency levels as a function of the environmental reduced pressure as presented in Figs. 6 and 7. The sharp increase in the fatigue life ratio in the critical zone can be attributed to the transition in fatigue behavior produced by competing adsorption and crack extension rates.

An increase in cyclic frequency should act to increase the real time rate of crack extension, thus shifting the adsorption-extension rate cross-over point or critical pressure value to higher pressure levels. In the critical pressure region, therefore, the measured fatigue life will be extremely sensitive to the cyclic frequency level and relatively small changes in loading rate may result in relatively major changes in fatigue life. At pressure levels well above or below the critical zone, changes in the time rate of crack extension due to changes in cyclic

frequency will generally not be sufficient to translate the critical pressure level to the operating pressure level. Hence, the frequency effect would be expected to assume the normal condition usually encountered at unit atmosphere.

According to this interpretation, similar frequency effects can be expected at operating pressure levels above or below the critical pressure zone. Within the zone, however, relatively large changes in fatigue properties with frequency can be anticipated. The experimental results obtained in this investigation appear to be in good agreement with this explanation.

PHASE II

TENSILE FATIGUE EXPERIMENT

INTRODUCTION

As noted previously, both rewelding of the fatigue crack surfaces and internal stress relief by means of dislocation escape at free surfaces in the absence of an adherent oxide barrier film have been advanced to account for the retardation of the crack growth rate in vacuum. Rewelding of oxide-free surfaces presumably may occur during the compressive portion of an alternating stress cycle. Accordingly, it was considered instructive to devise a fatigue test in which a specimen with an induced crack was maintained under an alternating tensile strain amplitude such that the fatigue crack would not be compressively loaded. In this way, contact between fracture surfaces at the tip of the crack would be minimized and the crack front would be continuously exposed to the outer gas environment.

In order to carry out this experiment, it was found necessary to design a tensile fatigue fixture and a plane sheet specimen configuration since preliminary work with the bend stress mode showed that flexure specimens generally deformed under repeated half-cycle bending loads to approximate the reverse bending or alternate tension-compression stress distribution. The tensile fatigue fixture and sheet specimens were designed to be incorporated in the existing Unit I assembly.

EXPERIMENTAL PROCEDURE - PHASE II

Tensile Fatigue Apparatus

In order to carry out alternating tensile stress tests on sheet specimens of 1100-H14 aluminum in vacuum, the Unit I vacuum fatigue apparatus was extensively modified to incorporate a four-station tensile loading fixture. A massive cylindrical support frame shown in Fig. 8 was designed to be rigidly attached to the original bend specimen base. The copper-plated steel frame supported the fixed lower end of the tensile specimens as shown in Fig. 9 such that the specimens were aligned axially with the crank shafts. The upper ends of the specimens were connected via a flexible spring steel coupling to four of the crank shafts penetrating through the vacuum flange plate. In this manner, the original motor driven eccentric cam housings were utilized for converting the vertical alternating motion of the shafts into a tensile strain amplitude.

Interior lighting and angular reflectors were provided for each station to permit direct observation of the specimen gauge sections through the individual view ports on the vacuum flange. In addition, each specimen was incorporated into a sensitive relay circuit which automatically stopped the motor drives upon fracture and separation of the specimens.

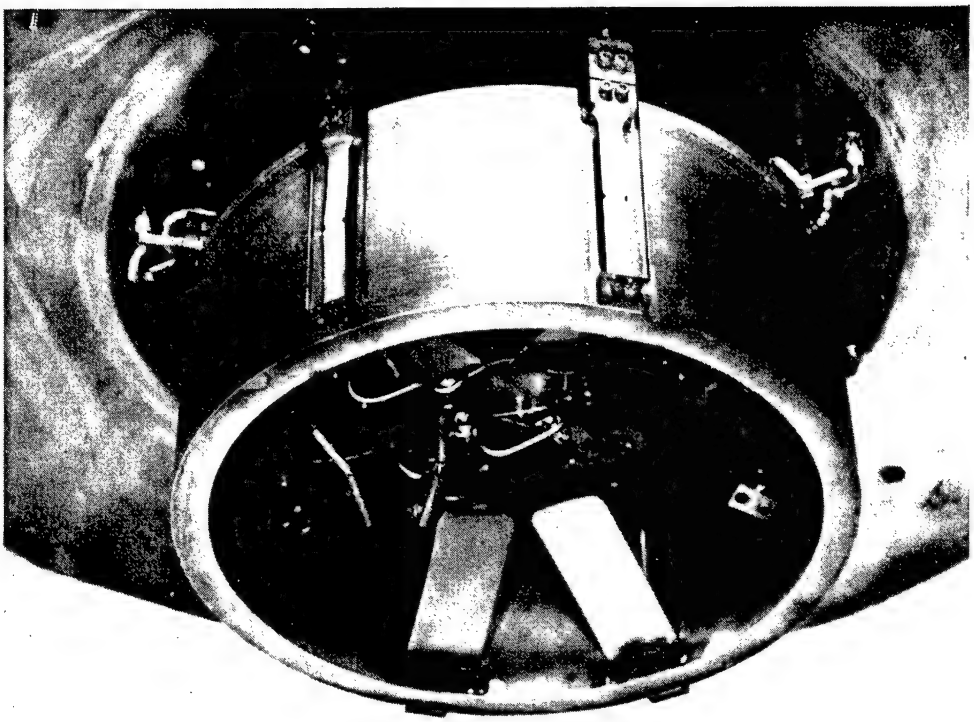

Tensile Fatigue Apparatus Mounted
On Vacuum Flange Plate Of Unit I
Fatigue Tester.

Fig. 8

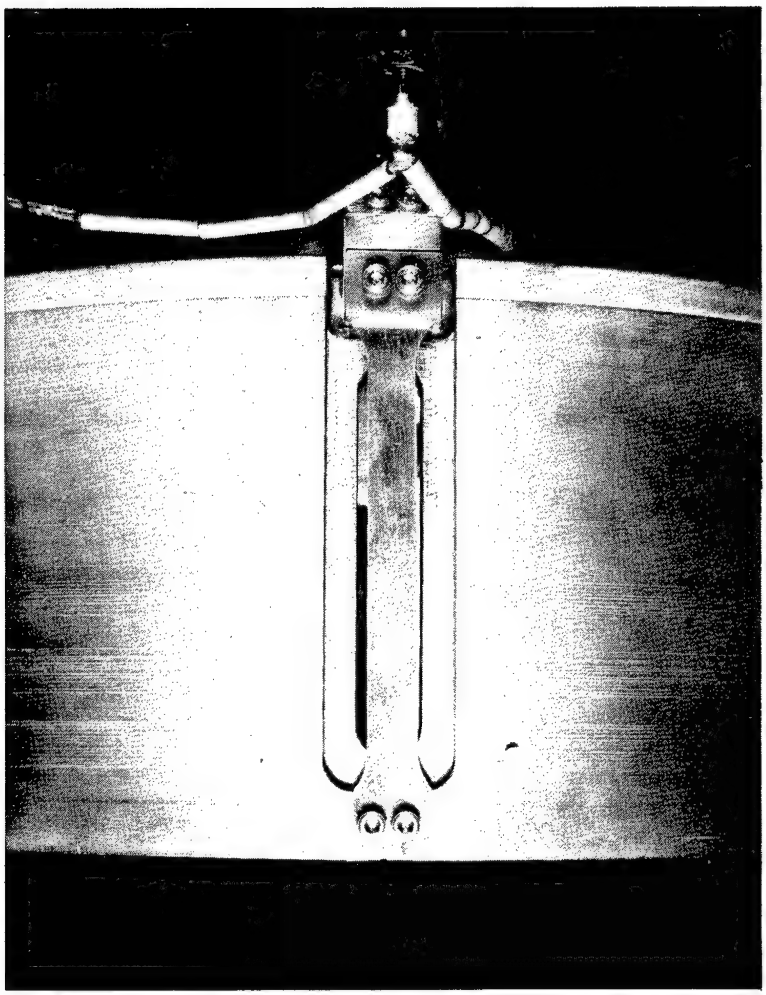

View Of Tensile Fatigue Specimen
Positioned In Fatigue Unit.

Fig. 9

The tensile fatigue fixture was designed to test plane sheet specimens with the configuration shown in Fig. 10. Consisting of a thin sheet 0.016 in. in thickness with a gauge section 3.5 in. long and 0.375 in. wide, the specimens were pre-notched with side-edge cuts giving a stress concentration factor of about 2.43 at the center of the specimen gauge section. The notched configuration was chosen to induce early crack initiation in the observable portion of the specimen length.

For a net specimen cross-sectional area of about 5×10^{-3} in.^{2} and a gauge length of 3.5 in., a set of eccentric cams providing 4.8×10^{-3} in. total deflection were fabricated and installed in the bearing support housings. The total resultant tensile strain amplitude of about 1.37×10^{-3}, co-responding to a peak alternating net section stress of about 13,700 psi for 1100 aluminum, required a peak alternating load of approximately 70 pounds force imposed by the crank shaft. Under these load and deflection conditions, the crank shaft, couplings and base frame were designed to limit elongation errors to less than 2×10^{-5} in. yielding a total error in tensile elongation of about 0.4 per cent.

Tensile Fatigue Test Procedure

After some preliminary experimenting, a satisfactory specimen design and testing procedure was envolved. The specimens were loaded into the fatigue stations with the eccentric cams adjusted to their lower limit of motion corresponding to the minimum specimen extension. After proper alignment, the specimens were extended by imposing a constant tensile load of about 5 pounds corresponding to a tensile stress of approximately 1000 psi. The constant load was maintained by adjustment of the bearing housing supporting the eccentric and crank shaft. Revolution of the cam through its total 0.0048 in. eccentricity then produced a tensile stress cycle alternating between extremes

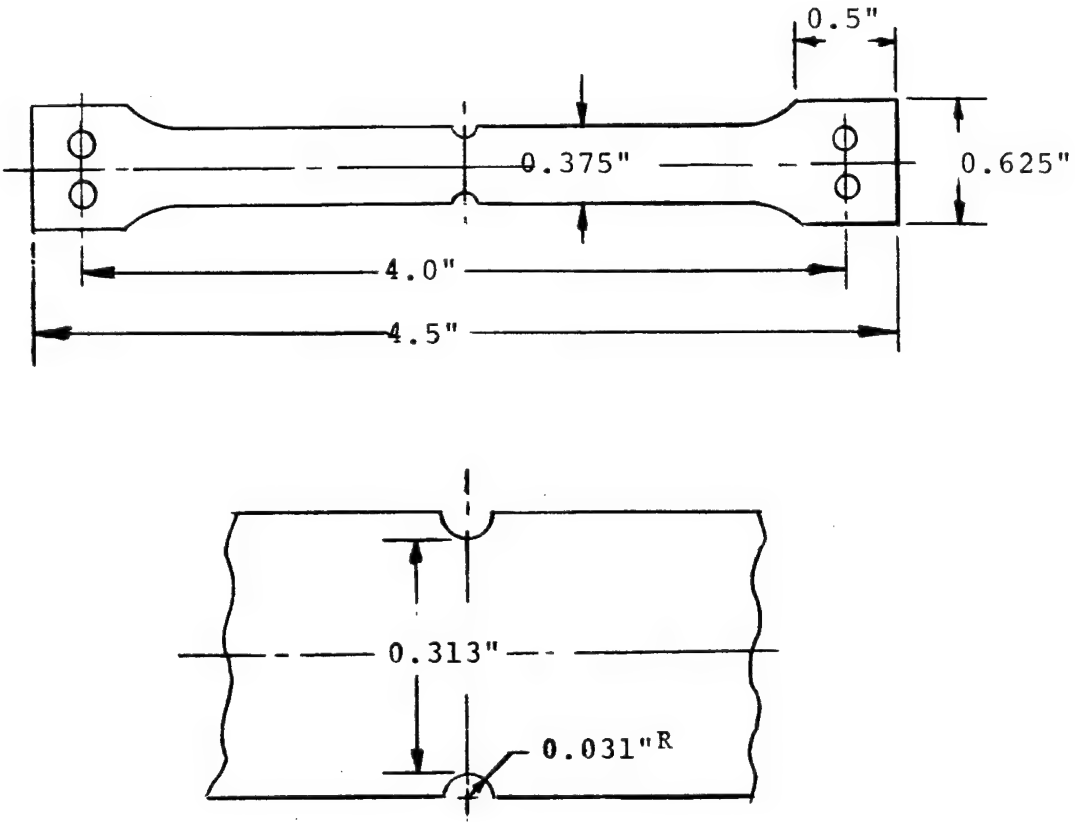

Fig. 10 Detail of tensile fatigue specimen.

of 14,700 and 1000 psi. The actual tensile strain limits were 1.47×10^{-3} and 0.1×10^{-3} so that the specimen was not subjected to gross compressive strains during fatigue crack propagation.

After initially fatiguing about 1000 cycles, the tests were interrupted and the specimens checked to ensure that the imposed constant stress was maintained. Generally, a limited amount of strain relaxation was noted due to specimen creep and yielding at the grips.

In fatigue operation, a set of four sheet specimens were fatigued at constant strain amplitude and standard pre-load in air until perceptable crack nucleation occurred in the side notches. The fatigue assembly was then placed in the vacuum system and evacuated under ion pumping. In the vacuum environment, three of the stations were reactivated and the specimens were fatigued to fracture. The fourth specimen was tested completely in air for comparison. Care was taken to prepare each set of four specimens in as nearly identical a condition as possible.

EXPERIMENTAL RESULTS - PHASE II

Fatigue tests were conducted at 5 cycles/sec with a tensile strain distribution alternating between 0.1 and 1.5×10^{-3} strain as outlined above. The tests were initially run in air until fatigue crack nucleation at the specimen edge notches was detected. The tests were then interrupted and continued after evacuation to vacuum levels in the range 5×10^{-6} to 8×10^{-7} torr. Several control specimens were fatigued to failure completely in the air environment in order to compare to the low pressure data.

The results of two representative test programs are given in Fig. 11. In this illustration, the number of tensile strain cycles to induce a detectable fatigue crack in air is denoted an N_I (A); the number of additional cycles to propagate the crack to total failure in vacuum and in air is denoted as Np (V) and Np(A), respectively. The results shown are test averages for two test series with specimens prepared to yield slightly varying notch induced stress concentrations.

A representative fatigue crack, interrupted during the course of a test, is shown in Fig. 12. Initiating at the base of the machined notch, the crack front has propagated a distance of 0.018 in. across the specimen cross-section before interruption. It is evident that the cyclic applied stress has generated a localized plastically deformed zone ahead of the crack front. The rate of crack extension may be expected to be related to the intensity of deformation and plastic flow preceding the crack.

It is evident that the introduction of a vacuum environment had a substantial influence on the subsequent growth rate of induced fatigue cracks. For the strain levels used in these experiments, an approximately six-fold increase in the number of strain cycles to cause fracture in vacuum to that in air was observed, indicating a marked reduction in fatigue crack growth comparable to prior results obtained in reverse bending.

These results inferred that variations in mean stress level, crack exposure time, and fracture surface contact had a minor effect on the fatigue crack-atmosphere interaction. Fatigue crack retardation in vacuum can be expected with widely varying alternating stress configurations.

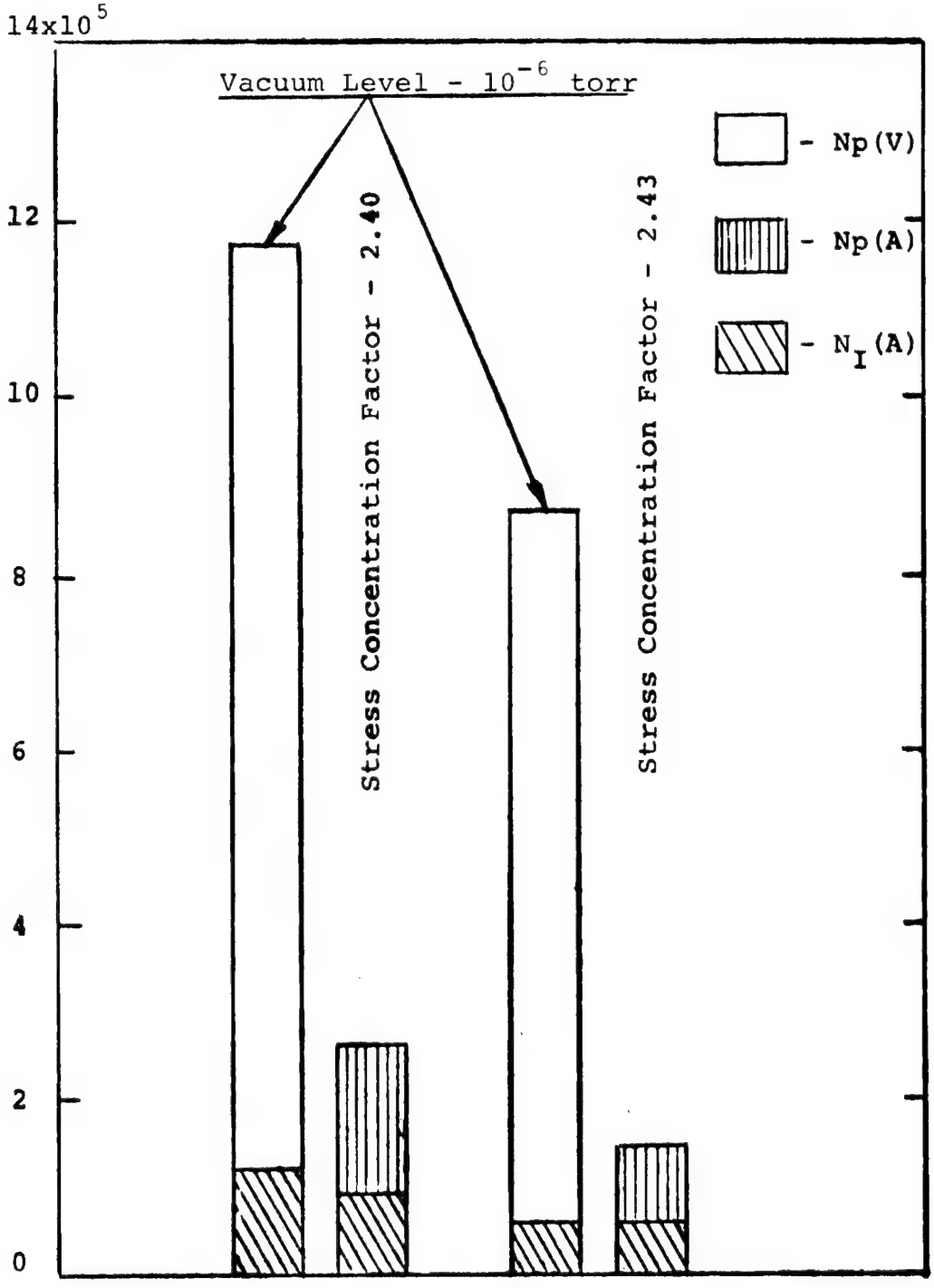

Fig. 11 Effect of 10^{-6} torr vacuum environment on the fatigue behavior in tensile fatigue stressing.

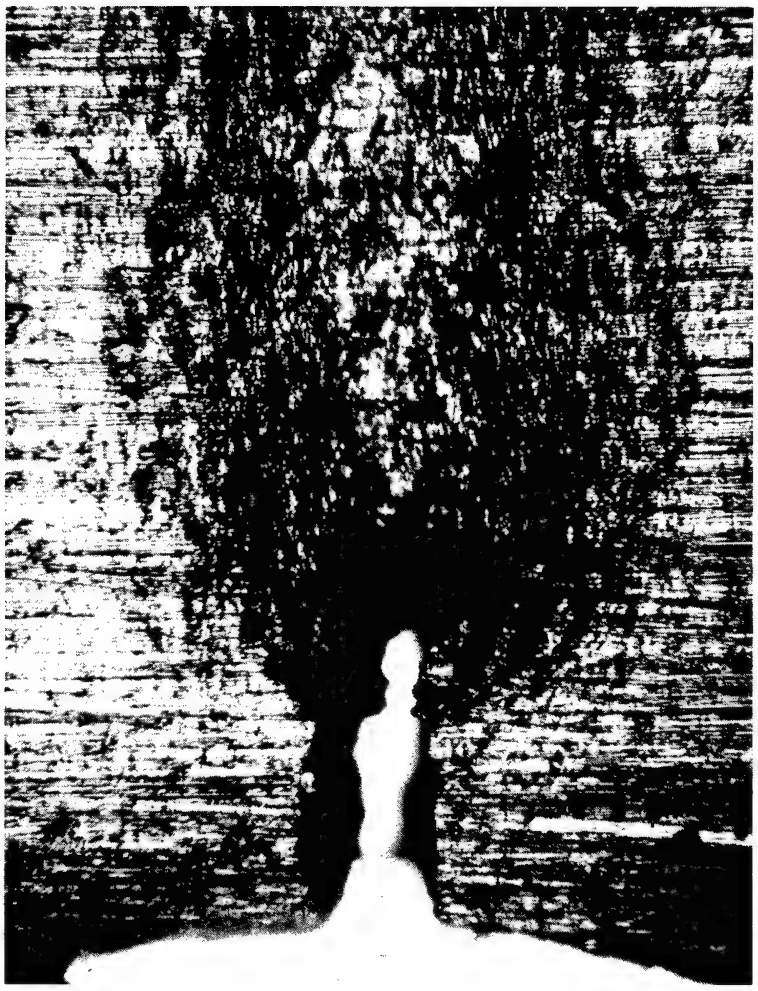

Detail Of Fatigue Crack Originating At Notch And Propagating Into Tensile Specimen Cross-section. Note Plastically Deformed Zone Ahead Of The Crack Front 75X.

Fig. 12

DISCUSSION - PHASE II

Assuming that fatigue crack closure and fracture surface compressive contact at the crack root are effectively minimized under conditions of alternating external tensile elastic strain, the results obtained by the present tests would appear to indicate that crack growth retardation in vacuum does not primarily occur through a fracture surface rewelding mechanism. Cold welding experiments in vacuum have generally shown that large scale metallic adhesion requires considerable plastic compression at the interface in addition to the absence of adsorbed surface contaminants.[8] Although the local surface stress distribution at the crack root cannot be precisely estimated, the presence of high plastic compressive stresses at the fracture surfaces under conditions of externally applied tensile straining would be unlikely.

In the absence of a surface rewelding mechanism, crack retardation may be attributed primarily to the relief of plastic stress in a localized zone about the crack tip by means of dislocation escape at the oxide-free surface initially created during crack extension. The dislocation excape mechanism under conditions where oxide-free surfaces have been maintained by continuous electrochemical dissolution, has been observed to produce marked increases in ductility and to retard the build-up of fracture inducing stresses.[9]

PHASE III

THE EFFECT OF SUBGRAIN SIZE

INTRODUCTION

The application of a fatigue stress to a metallic material causes a multiplication and redistribution of internal defects. Vacancy sites are known to be generated within the metallic lattice and dislocations are also created.[10] The dislocations generated within most pure metals tend to arrange themselves into high density walls which delineate areas that contain very few dislocations. The individual areas that are bounded by this dislocation network, which is three dimensional, are called subgrains.

Pratt[11] presented the results of investigations on copper which indicated that a correlation existed between the diameter of the subgrains produced dynamically within a metal and the applied fatigue stress. Working with anealed material it was noted that the largest stresses produced the smallest subgrain diameter. If the value of the stress were changed during a fatigue test the subgrain diameter was also observed to change. The results of a later study[12] indicated that similar atomic rearrangements occurred in aluminum. A true correlation of the effect of subgrain size on the fatigue crack growth rate could not be estimated from the results of the above work since all the tests were conducted in an air environment, the corrosive action of which would seriously effect the observed crack growth rates.

In the following sections experiments are described in which the subgrain size generated in aluminum was determined at various fatigue stress levels. Stress-corrosion effects were absent, since the tests were carried out at reduced pressures below the critical pressure for transition. A true correlation between applied stress, subgrain size and crack growth rate was therefore obtained.

EXPERIMENTAL TECHNIQUES - PHASE III

Fatigue Tests

Fatigue tests were carried out in Unit I at vacuum levels about 2×10^{-17} torr at constant flexure amplitudes designed to produce surface stress values of 11,400 and 18,200 psi. The corresponding average cyclic life ranges with a bending rate of 50 cycles/sec were approximately $5.0 - 5.5 \times 10^6$ and $0.15 - 0.66 \times 10^6$ cycles, respectively. For several specimens, the fatigue tests were conducted after pre-stressing to selected values. The tests were performed on 1100 aluminum in the as-received H14 rolled condition (50 per cent reduction in area) and also after annealing at 500°C for 1 hour in argon.

After fatiguing to fracture, the specimens were prepared for metallographic and electron microscopy examination. Areas of interest included the fracture surfaces and regions immediately adjacent to the fracture path.

Foil Preparation

Thin film specimens suitable for examination in the electron microscope were prepared using combined mechanical and

electropolishing techniques. The surface of the fatigued specimen was removed using a jeweler's saw. The resulting slice, which was 0.025 in. thick, was thinned to 0.005 in. by grinding under water with successively finer grades of polishing papers. Only very small loads were applied to the specimen during the polishing operation to minimize the introduction of mechanical damage or heat into the specimen.

The foils produced by the sectioning treatment were further thinned by using an electropolishing technique. The foil edges were coated with a non-conducting film before the specimen was immersed in the electropolishing solution. Various electrolytes were investigated; however, polishing in a solution of perchloric acid and alcohol at 0°C tended to produce foils of the most consistent quality. The maintainance of the correct temperture was found to be important, for an excessively high temperature resulted in a thick oxide film being formed on the specimen surface, while a low electrolyte temperature resulted in long polishing times.

Electropolishing was carried out using an applied voltage of 20 volts and a current density of 0.2 amp/cm^2 until perforation of the foil occurred. The specimen was then removed from the solution, the edges of the perforation were laquered and the electropolishing was restarted. These steps were repeated until eventually two holes appeared simultaneously in the foil. Specimens suitable for examination in the electron-microscope could then be cut from the material that bridged the two holes.

The thin films were sandwiched between the two halves of a commercially available "clam shell" grid before being examined in a Hitachi electron microscope operating at an accelerating voltage of 100 KV.

Subgrain Diameter Determination

The mean subgrain diameter was determined by measuring the number of boundaries intersected by a line of known length. Specifically, a number of parallel lines were superimposed on photomicrographs taken at random from a thin film. The total number of subgrain boundaries intersected by the lines was counted, after which the grid was rotated 15 and a further count was made. This process was repeated until the lines were rotated through 90°. The mean subgrain diameter (d) used was then calculated from the expression.

$$d = \frac{N_1+N_2+N_3---N_i}{n_1+n_2+n_3---n_i} \qquad (1)$$

where N_i is the length of the ith line and n_i is the number of subgrain boundaries cut by the ith line.

EXPERIMENTAL RESULTS AND DISCUSSION - PHASE III

Constant Stress Tests

The application of an alternating stress to a metallic specimen has been shown to produce an increase in the number of dislocations and vacancies distributed throughout a metallic lattice. The relative geometry of these defects has also been shown to be altered, since dislocations tend to arrange themselves into highly dense networks surrounding areas that contain very few imperfections. These low density dislocation areas are termed subgrains.

In this investigation two material conditions were studied for 1100 aluminum; H14 cold rolled (50 per cent reduction in area) and "0", fully annealed. The typical dislocation distributions are shown in Figs. 13 and 14. The annealed material contained long dislocation lines randomly distributed throughout the bulk of the material with no subgrains observed. The dislocation arrangement that existed within the work hardened material was strikingly different for the dislocations were distributed in definite well defined subgrain boundary arrays with a mean average diameter of 1.14μ.

The application of a fatigue stress at constant strain amplitude to both the above materials caused marked changes to occur in the defect arrays within the metallic lattice. Subgrain boundaries were generated within the annealed material, while those present in the hardened material increased in size. Typical fatigue formed subgrains are shown in Fig. 15. In this figure, subgrain boundary walls are seen to consist of long dislocation lines stacked on top of each other, a process which results in the formation of typical large angle boundary. In another part of the same specimen heavily jogged dislocations are observed forming themselves into the same type of arrangement. In various areas of the specimen, subgrains were observed which were elongated in one principal direction, as shown in Fig. 16.

The relationship between the applied stress and the cyclic fracture life for initially annealed and for hardened specimens is shown in Fig. 17. The fracture life was always greater for specimens fabricated from the cold worked material, but the magnitude of this difference progressively decreased as the value of the applied stress was raised. The value of the applied stress sensitively effected the equilibrium subgrain diameter; the largest applied stress produced in the annealed material the

Representative Dislocation Arrays
In Annealed Aluminum 58,000X.

Fig. 13

Representative Dislocation Subgranular Structure In Cold Worked 1100-H14 Aluminum 39,000X.

Fig. 14

Well Defined Dislocation Subgranular Structure Formed In 1100-H14 Aluminum Fatigued With A Stress Amplitude Of 13,600 psi. Average Subgrain Size Is About 2.0μ 14,000X.

Fig. 15

Elongated Subgrain Texture Observed In 1100-0 Annealed Aluminum Fatigued With Surface Stress Amplitude Of 11,400 psi.

Fig. 16

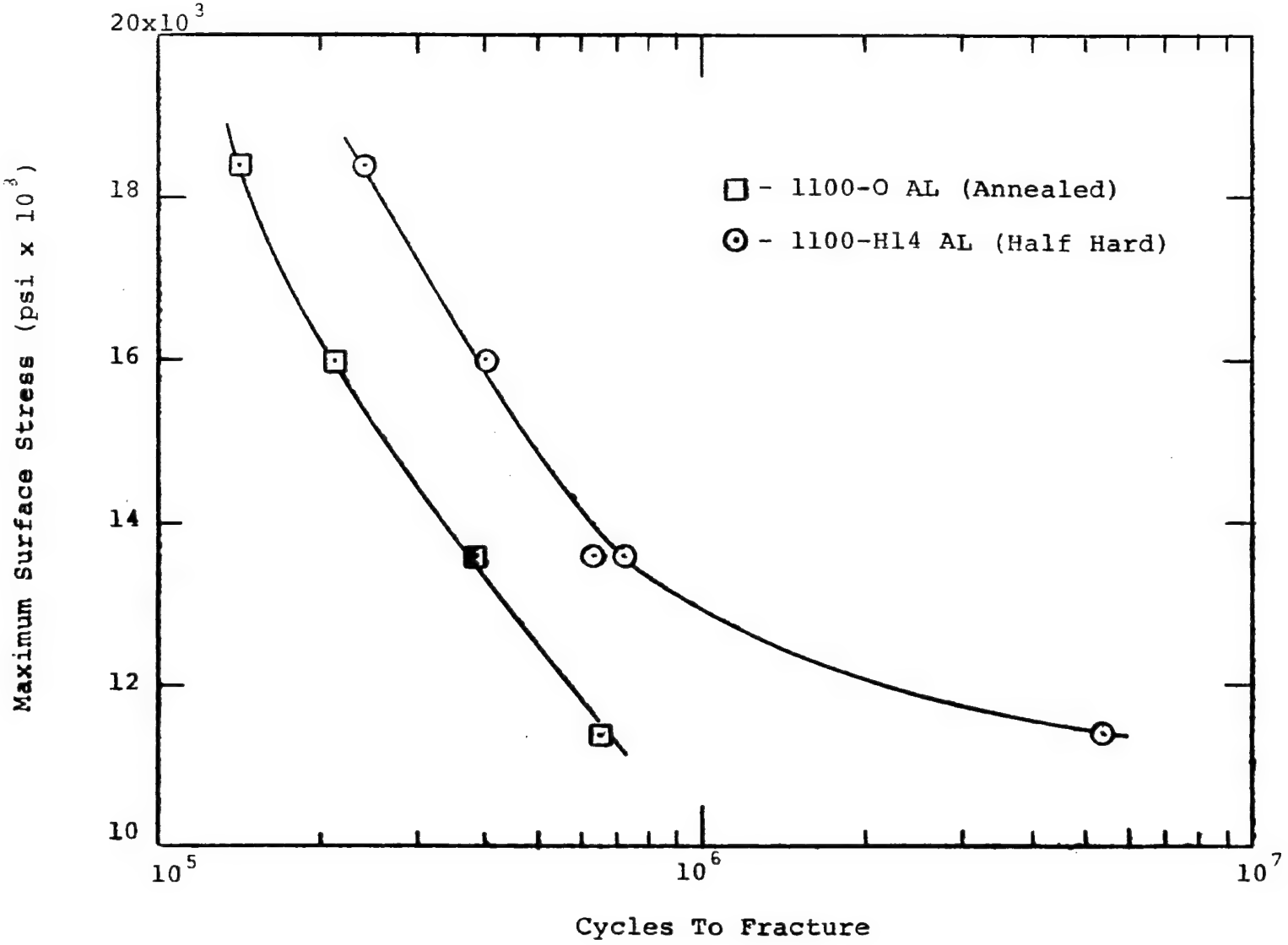

Fig. 17 Effect of prior cold work on the fatigue properties of aluminum

smallest subgrains; conversely an identical stress produced the largest subgrains within the hard material. This effect is graphically illustrated in Fig. 18. It should be noted that the subgrain size generated within the annealed specimens for the largest stresses applied approached but never equaled that generated within the half hard material.

In a previous paragraph it was pointed out that the fatigue resistance of metallic materials can be increased if specimens are fabricated from source material previously subjected to a cold working operation. Techniques such as rolling or forging effectively harden the material by raising its flow stress. The strengthening effects obtained, while appreciable at low fatigue stress levels, become less significant at high alternating stress levels since the original subgrain size and hence the flow stress of the material are substantially changed. In the case of a metal subjected to a large fatigue stress, the change in hardness that occurs during the course of a test can be appreciable and can negate the beneficial effects of the prior cold working operation. Fatigue micro-hardness valves obtained for the materials investigated here were determined using a Leitz micro-hardness tester and are also shown in Fig. 18. It is interesting to note that fatigue stresses can either soften or harden the metallic lattice; which effect will predominate is solely dependent on the initial condition of the material. Further, the linear relationship obtained between the hardness and the generated subgrain size suggest that the flow stress is largely dependent on the subgrain diameter; the mechanism by which the observed subgrain size is generated appears to be relatively unimportant.

Since the generated subgrain size is dependent on the value of the applied fatigue stress, it is difficult to associate the crack growth rate with any particular subgrain size. However, for a given applied stress the subgrain size generated in initially

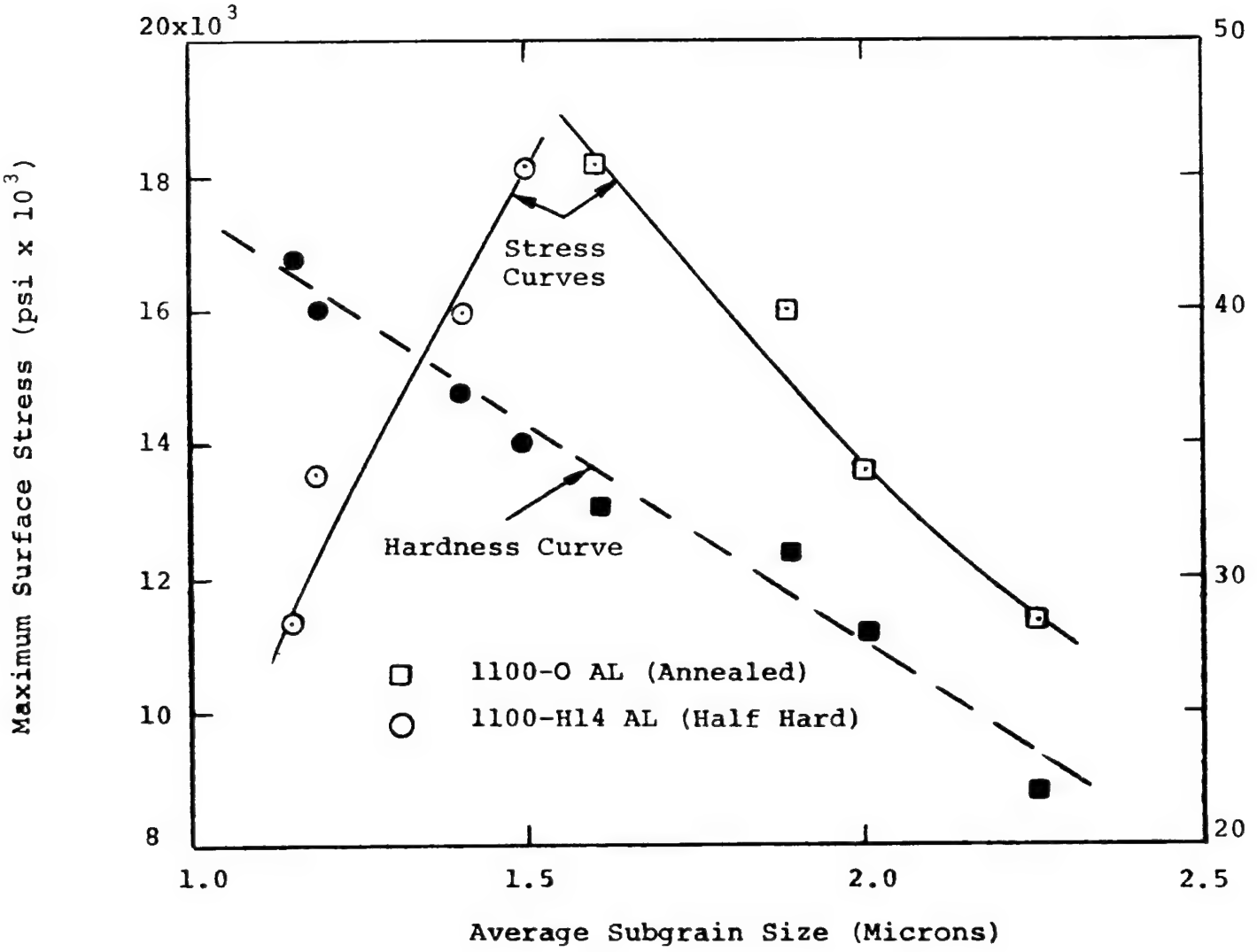

Fig. 18 Dependence of the fatigue subgrain size on applied stress amplitude and hardness level.

hard or annealed material was different; thus a comparison could be attempted. The crack growth data, summarised graphically in Fig. 19, were used to estimate the crack growth rate through the first ten per cent of the fracture life. In Fig. 20 the resultant crack growth rate is shown for various subgrain sizes, each connected point denoting an equal stress condition. It is to be noted that the generated subgrain size appeared to sensitively control the fatigue crack growth rate while observation of the data indicated that appreciable fatigue strengthening could be obtained within a given material if the original subgrain size could be prevented from growing larger.

Variable Stress Tests

The effect of variations in the magnitude of the stress applied to a specimen during the course of a test was studied. Tests were carried out using specimens prepared from both cold worked and annealed material. Initially, two control groups of eight specimens each prepared from both materials were fatigued to fracture at a constant stress. The variable stress experiments were then carried out by first subjecting a specimen to a number of stress cycles sufficient to initiate a crack. The crack was then propagated at a different stress until fracture of the specimen occurred. Two series of tests were conducted on each material; in one series the crack was initiated at 18,200 psi surface stress and propagated at 11,400 psi; in the second series the crack was initiated at 11,400 psi and propagated at 18,200 psi.

A statistical comparison of the results given in Table II shows quite clearly that the initial pre-stress had an insignificant effect on the total fatigue life of an aluminum specimen.

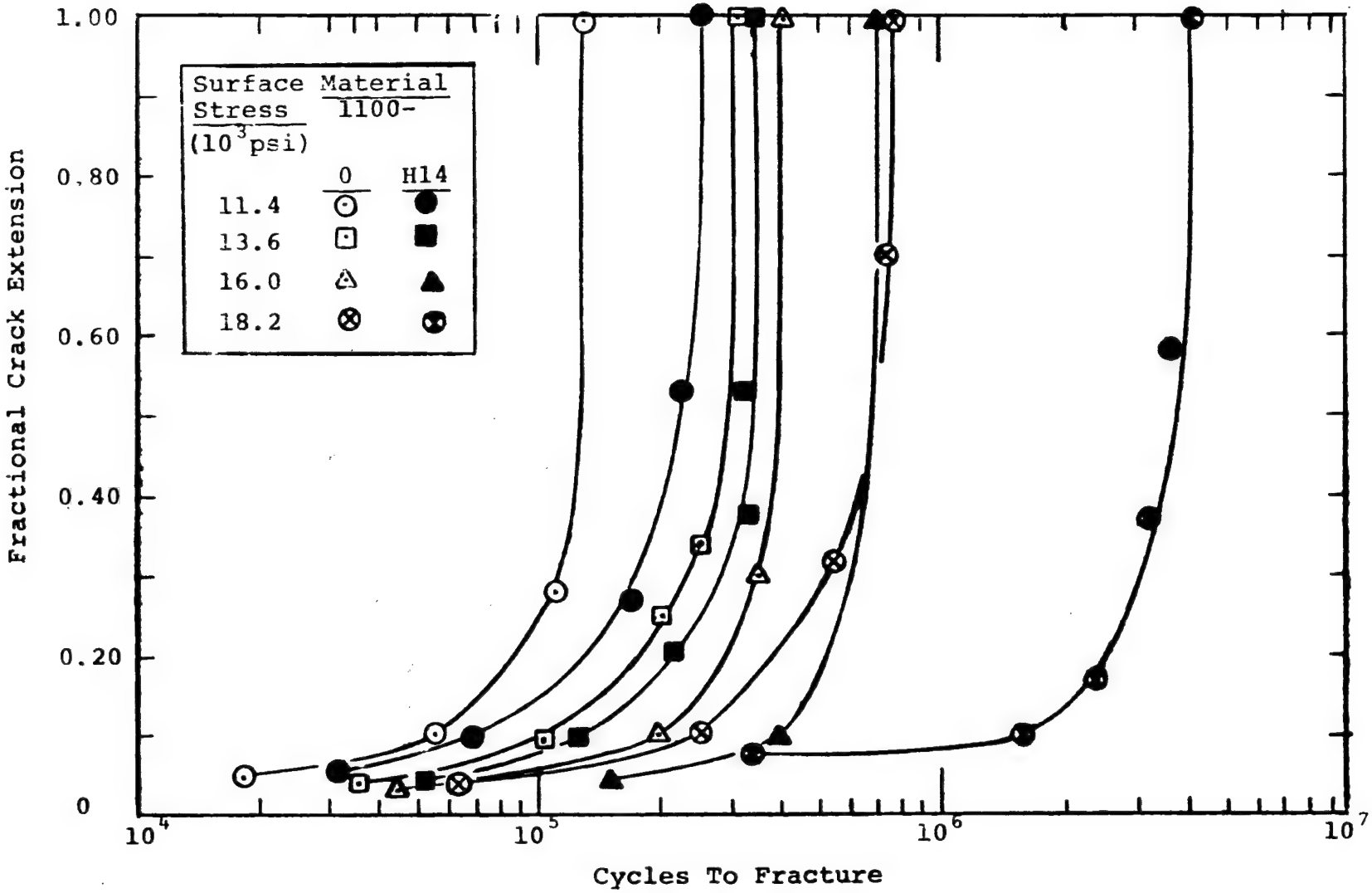

Fig. 19 The dependence of the rate of crack extension on and the number of cycles to fracture on applied stress amplitude.

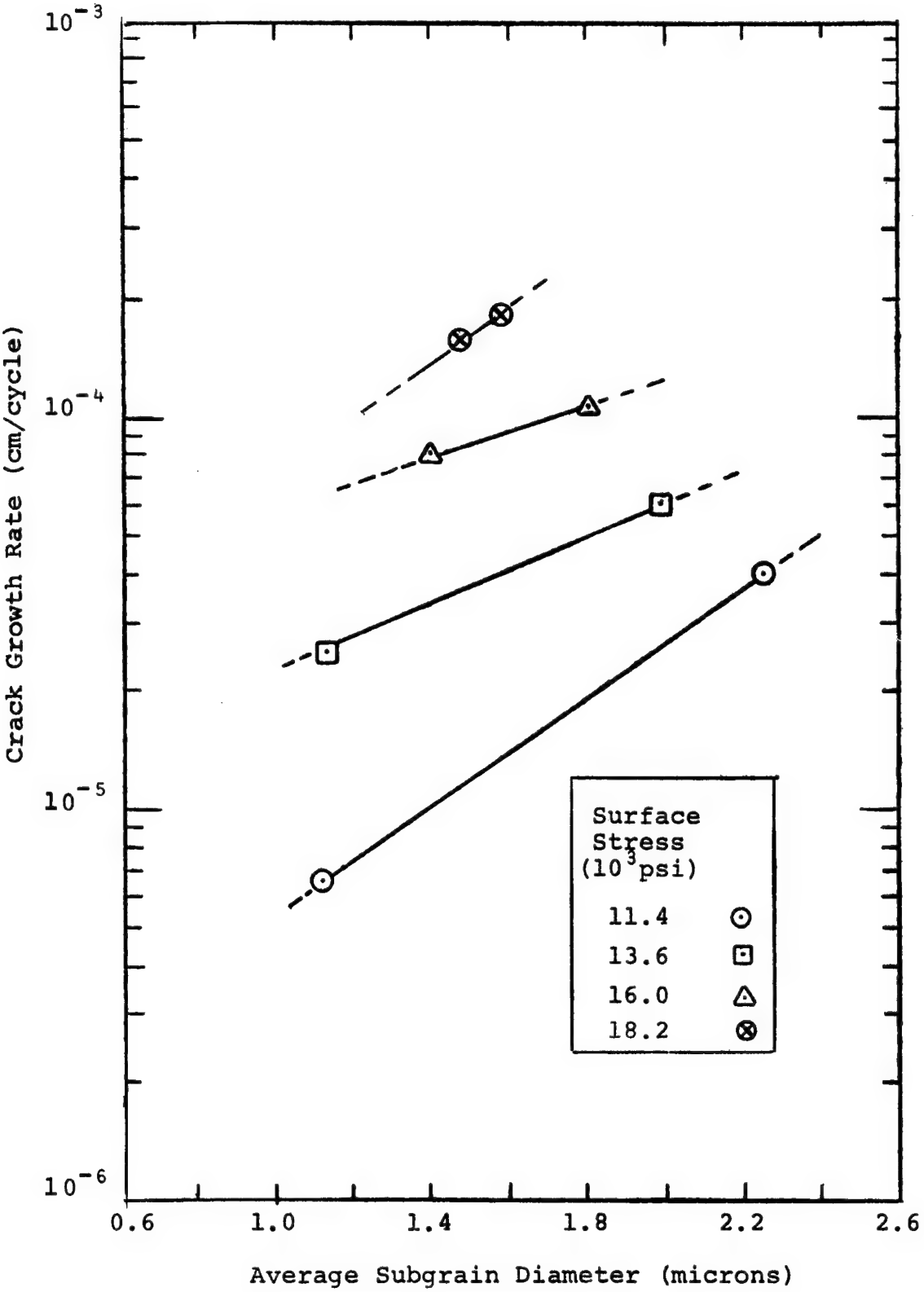

Fig. 20 The effect of the subgrain diameter on the observed crack growth rate.

TABLE II

EFFECT OF STRESS VARIATION ON THE FATIGUE LIFE ON ALUMINUM IN A VACUUM OF 10^{-7} TORR

STARTING CONDITION	PRESTRESS ($\times 10^3$ psi)	FINAL STRESS ($\times 10^3$ psi)	AVERAGE LIFE (Cycles x 10^6)
Annealed	0	11.4	.64
Annealed	18.2	11.4	.66
Annealed	0	18.2	.14
Half Hard	0	11.4	5.0
Half Hard	18.2	11.4	5.5
Half Hard	0	18.2	.24
Half Hard	11.4	18.2	.19

Specimens fabricated from both annealed and half hard material behaved in essentially the same manner. Previous work has shown that the application of fatigue stresses to aluminum quickly generates internal subgrains which grow to a specific diameter. It has also been reported that the size of the subgrains generated by a prior fatigue stress would rapidly change if a stress of sufficiently different magnitude was subsequently applied. It can be inferred therefore that for an initially annealed material the effect of a prestress on the fatigue life of a material should be small. The results obtained in this work substantiate this conclusion.

In a previous section, it has been reported that a small fatigue stress fails to modify the initially small subgrain size present within cold worked material. Thus, a prestress of small magnitude would not be expected to modify the subsequent fatigue life experienced by a specimen subjected to a large stress. However, a large prestress would be expected to appreciably change the initial subgrain size of hardened material. Thus, a subsequently applied low fatigue stress should propagate a crack at a rate appreciably greater than that exhibited by a non-prestressed specimen. Reference to Fig. 20 suggests that a minimum increase in crack growth rate of about two should be exhibited for the stress levels employed here.

The reason for the generally small magnitude of the effect observed in this work is not entirely clear, but could be associated with the geometry of the testing procedure. The outer fiber of a bend test specimen is the only portion of the test piece that experiences the maximum strain; thus subgrain growth effects will rapidly decrease from the outer to the inner fibers. Further tests would be required, using a test piece stressed equally across its area, in order to substantiate the magnitude of the effect.

CONCLUSIONS

From the results of the current work, the following conclusions may be advanced:

1. The effect of the cyclic rate of straining in fatigue can be interpreted by the crack adsorption mechanism postulated in prior work to account for crack retardation in the absence of oxygen or water vapor gas concentrations. In the vicinity of the critical pressure value for fatigue transition, an increase in the cyclic frequency will increase the intrinsic time rate of crack growth, thus shifting the critical pressure to higher values. At operating pressures about 10^{-2} to 10^{-3} torr, therefore, an increase in cyclic frequency for aluminum will result in a marked decrease in the rate of crack growth.

2. The decrease in the crack growth rate at low pressures below the critical zone does not appear to result from the re-welding of clean fracture surfaces during the alternating stress cycle since the usual retardation effect was observed under conditions of tensile loading in which crack surface recontact and closure would be substantially minimized. The change in crack growth rate in vacuum may be attributed to dislocation escape at oxide free crack surfaces, acting to relieve the defect induced stress concentration in the deformed zone ahead of the crack front.

3. Fatigue stresses generated a characteristic subgranular structure comprising dislocation boundary networks. For initially annealed aluminum with no well defined substructure, the fatigue induced subgrain size will vary inversely with applied stress amplitude. With initially hardened aluminum, the characteristic subgrain distribution generated by plastic deformation will be changed under fatigue stressing, the final subgrain size approaching the annealed state values, particularly at higher

stresses. Changes in the magnitude of the applied fatigue stress during the course of a test will induce corresponding changes in the final subgrain size.

FUTURE WORK

The following suggestions are outlined for extending the current series of investigations on the effect of reduced gas pressures on the fatigue behavior of metals.

1. The investigations conducted during the three year program concluded in this report on the fatigue properties of 1100 aluminum in vacuum should be extended to additional materials including 2024 and 7075 aluminum alloys, titanium -6Al-4V alloy, 304 stainless steel and several structural steel grades.

2. In particular, the effect of various residual gas compositions should be studied in the critical partial pressure range extending from 10^{-1} to 10^{-4} torr on the materials specified.

3. A detailed electron microscopic and metallographic examination of the fatigue fracture mechanism in the absence of corrosive gases should be carried out for various metals of interest.

4. The effect of various inorganic and polymer protective surface coatings on the fatigue response in air and in other corrosive environments should be conducted on materials of engineering interest.

REFERENCES

1 M. E. Reed and M. J. Hordon, "Fatigue Apparatus for Extreme High Vacuum", Rev. Sci. Instr., Vol. 38, 1967, p. 322.

2. M. A. Wright and M. J. Hordon, "Effect of Residual Gas Composition on the Fatigue Behavior of Aluminum", (to be published in Transactions TMS-AIME), 1968.

3. M. J. Hordon and M. E. Reed, "A Study of the Mechanism of Atmospheric Interaction with the Fatigue of Metals", NASA CR-68036 (Contract NASw-962), Sept. 1965.

4. M. J. Hordon, M. A. Wright and M. E. Reed, "Mechanism of the Atmospheric Interaction with the Fatigue of Metals", NASA CR-82446 (Contract NASw-1231), Sept. 1966.

5. M. J. Hordon, "Fatigue Behavior of Aluminum in Vacuum", Acta Met., vol. 14, 1966, p. 1173.

6. M. A. Wright and M. J. Hordon, "Temperature Dependence of the Fatigue Transition Pressure for Aluminum", Acta Met., vol. 15, 1967, p. 430.

7. A. J. Kennedy, "Processes of Creep and Fatigue in Metals". John Wiley & Sons, Inc., New York, 1963, pp. 313-316.

8. M. J. Hordon, "Adhesion of Metals in High Vacuum", ASTM-ASLE Symposium on Cold Welding on Adhesion or Materials in The Space Environment, Toronto, 1967, (to be published as ASTM-STP 431, Symposium on Cold Welding or Adhesion of Materials in the Space Environment, Amer. Soc. for Testing Mat., Phila., 1968)

9. I. R. Kramer, "The Effect of Surface Removal on the Plastic Behavior of Metals", Transactions TMS-AIME, vol. 227, 1963, p. 1003.

NASA-Langley, 1968 — 17 CR-1165

NATIONAL AERONAUTICS AND SPACE ADMINISTRATION
WASHINGTON, D. C. 20546

OFFICIAL BUSINESS

FIRST CLASS MAIL

POSTAGE AND FEES PAID
NATIONAL AERONAUTICS AND
SPACE ADMINISTRATION

"The aeronautical and space activities of the United States shall be conducted so as to contribute . . . to the expansion of human knowledge of phenomena in the atmosphere and space. The Administration shall provide for the widest practicable and appropriate dissemination of information concerning its activities and the results thereof."

—NATIONAL AERONAUTICS AND SPACE ACT OF 1958

NASA SCIENTIFIC AND TECHNICAL PUBLICATIONS

TECHNICAL REPORTS: Scientific and technical information considered important, complete, and a lasting contribution to existing knowledge.

TECHNICAL NOTES: Information less broad in scope but nevertheless of importance as a contribution to existing knowledge.

TECHNICAL MEMORANDUMS: Information receiving limited distribution because of preliminary data, security classification, or other reasons.

CONTRACTOR REPORTS: Scientific and technical information generated under a NASA contract or grant and considered an important contribution to existing knowledge.

TECHNICAL TRANSLATIONS: Information published in a foreign language considered to merit NASA distribution in English.

SPECIAL PUBLICATIONS: Information derived from or of value to NASA activities. Publications include conference proceedings, monographs, data compilations, handbooks, sourcebooks, and special bibliographies.

TECHNOLOGY UTILIZATION PUBLICATIONS: Information on technology used by NASA that may be of particular interest in commercial and other non-aerospace applications. Publications include Tech Briefs, Technology Utilization Reports and Notes, and Technology Surveys.

Details on the availability of these publications may be obtained from:

SCIENTIFIC AND TECHNICAL INFORMATION DIVISION

NATIONAL AERONAUTICS AND SPACE ADMINISTRATION

Washington, D.C. 20546